Tuning the colloidal stability in ionic liquids by controlling the nanoparticles/liquid interface

M. Mamusa, J. Siriex-Plénet, F. Cousin, E. Dubois, V. Peyre

Journal Name

COMMUNICATION

Tuning the colloidal stability in ionic liquids by controlling the nanoparticles/liquid interface

M. Mamusa,[a] J. Siriex-Plenet,[a] F. Cousin,[b] E. Dubois [a] and V. Peyre [a]

To shed light on the origin of colloidal stability in ionic liquids, we focus on a model colloidal system (maghemite nanoparticles) in which surface charge and counterion nature can be controlled at will. We thus evidence the crucial role of interfacial features on dispersion quality in a standard ionic liquid, ethylammonium nitrate.

Ionic liquids (ILs) are a novel class of solvents constituted solely of ions, with melting points below 100 °C. Although known for a long time, ILs have been attracting a great deal of interest in recent years due to some specific properties, such as non-flammability, negligible vapor tension and high thermal stability, to name a few. ILs are then promising "green" candidates that could replace classical and more dangerous organic solvents as reaction media in many fields, such as chemical organic and inorganic synthesis, enzyme-catalyzed reactions, or for the preparation of magneto-rheological fluids, lubricants and electrochemical devices.[1]

Initially used for chemical synthesis and electrochemistry, they have been more recently used as synthesis[2] media for several types of metal and non-metal nanoparticles. Although the possibility of obtaining stable colloidal dispersions or gels in ILs has been reported in literature, surprisingly, the state of dispersion of the nanoparticles obtained in the IL has not been thoroughly probed yet. A fine tuning of the state of dispersion is nevertheless crucial on an application point of view: whereas fully dispersed particles are needed for heterogeneous catalysis[3] or heat-transfer fluids,[4] controlled aggregation of particles to form physical gels[5] is required for Dye-Sensitized Solar cells[6] or gas sensors,[7] to cite a few.

In the few works on colloidal dispersions, stability was often ensured by using additives providing steric repulsions, such as polymers[8,9] or surfactants,[10,11] but a few studies also use pristine dispersions without any added molecules.[12,13] None of these works provide clear explanations with regard to the stability of the investigated systems, and this feature remains basically ill-understood.[9,14,15] Moreover, to our knowledge, no studies deal with the analysis of the relevant physico-chemical parameters controlling dispersion stability. In particular, the role of the particle/ionic liquid interface has never been properly investigated in colloidal systems.

The present work aims at examining the role of the surface state of nanoparticles on their colloidal stability in ILs; in order to do this, we focus on a model system for which the interface between the solid nanoparticles and the solvent can be modified, by tuning either the charge of the particles or the nature of their counterions.

The model system is based on a well-known aqueous colloidal dispersion of iron oxide magnetic nanoparticles. The stability of these suspensions can be tuned in water before the particles are transferred in ethylammonium nitrate (EAN), an IL considered as rather similar to water[16,17] and for which a large corpus of knowledge is currently available.

Let us first introduce the two components of the colloidal system studied in this work. Iron oxide nanoparticles were synthesized in the laboratory *via* the coprecipitation of iron ions in alkaline medium.[18,19] The maghemite (γ-Fe_2O_3) particles hereby obtained have a diameter around 10 nm and are dispersed in acidic aqueous medium (pH = 1.5). At this stage, the surface charge is positive ($Fe\text{-}OH_2^+$) and counterbalanced by NO_3^- anions. Such systems have been extensively studied as they are magnetic liquids, and they are commonly referred to as ferrofluids.[19-21]

Starting from these initial dispersions, several kinds of aqueous samples can be easily prepared. The surface charge can be tuned by changing the pH: the positive charge can vary from 2 e^-/nm^2 at low pH, down to 0 at the point of zero charge (PZC) located around pH = 7.0.[19] The nature of the anion (initially NO_3^-) can be modified in a process that requires passing through the PZC: the particles are flocculated at pH 7.0, and after thorough washing with water to remove the undesired ions, an acid with the desired anion (perchlorate or benzenesulfonate) is added.

If a stable maghemite dispersion is needed at neutral pH (for example, for biomedical applications), the limitations of the PZC can be overcome by the adsorption of citrate molecules, introduced as a citrate salt $[(^{-}OOCCH_2)_2C(OH)COO^{-}]X_3^{+}$. Here X^{+} becomes the counterion of the particles, and can be modified at will by introducing the desired citrate salt. In such systems, the particles have a negative surface charge of -2 e^{-}/nm^2 and the concentration of free citrate in the bulk is of the order of 0.01 mol L^{-1}.[21]

The second component concerned in this work is the IL solvent, ethylammonium nitrate (EAN), which was prepared by reacting equimolar quantities of nitric acid and ethylamine in distilled water[17] and purified according to a well-established protocol (see SI for details). At the end of the procedure the residual water content was determined *via* a coulometric Karl Fischer titration to be less than 0.3 wt% water. The EAN thereby obtained is a viscous, oily, odorless and transparent fluid, and its pH is slightly above 5 (*i.e.*, it is quasi neutral, as the autoprotolysis constant is pK_s=10 [16]). The pH measurements are performed in EAN by transposing the method classically used in water, with a glass electrode and a saturated calomel electrode as reference. Calibration is performed with three EAN solutions of pH 1.0, 5.4 and 9.0 (see Supplementary Information (SI) for all details on pH measurements and determination of the acidity constants of the citrate molecule in EAN).

Finally, we shall now see how these two systems, maghemite nanoparticles and ethylammonium nitrate, are mixed together. A volume V_{EAN} is added to a volume V_{aq_ff} of aqueous ferrofluid having a NP concentration of Φ_{NP} = 1%. The maximal volume fraction of the dispersed particles is thus 1% if $V_{EAN} = V_{aq\_ff}$, and 0.1% if $V_{EAN} = 10V_{aq\_ff}$. Water is then removed by freeze-drying, followed by stirring and sonication before further study. The step of mixing water and EAN leads to the formation of NP aggregates which, depending on the system, disappear completely, in part or not at all, after water removal.

The stability of these systems in EAN can first be assessed macroscopically through visual observation of the glass vials. Due to the strong absorption of visible light by maghemite nanoparticles, the suspensions are red and the intensity of such color provides qualitative indication about the volume fraction of dispersed particles (see examples in Figure 1).

Let us first examine the influence of the particles' surface charge on three types of systems:

-1) A sample containing uncharged flocculated particles at PZC in water (pH = 7) is also clearly unstable after the transfer to EAN (pH = 6; Figure 1, left): a floc is present at the bottom of the vial, and the supernatant is clear;

-2) Aqueous dispersions prepared at acidic pH with NO_3^{-} counterions are only partially stable upon transfer to EAN, meaning that only a fraction of all the particles can be dispersed, as evidenced by the presence of a reddish supernatant in coexistence with a precipitate. This type of sample will be referred to as "partial dispersion" in what follows. Also, a higher surface charge in water (*i.e.* lower pH) leads to a larger quantity of dispersed particles in EAN (Figure 1, middle);

-3) Aqueous dispersions prepared with citrate coating and Na^{+} counterions (neutral dispersions) also yield partial dispersions in EAN. However, in this case the dispersed fraction was much larger, and the remaining flocculated fraction was very low (so much as to be no longer visible in Figure 1, right). Please note that the supernatants were never turbid. Such results strongly suggest that particles maintain a surface charge in EAN, with the same sign as in water, and that uncharged particles cannot be dispersed in EAN.

The pH measurements show that, for acidic aqueous dispersions, the pH remains acidic in EAN, with $pH_{water} < pH_{EAN}$. This likely results from the loss of molecular HNO_3 or $HClO_4$ upon freeze-drying. As such loss cannot be avoided, very low pH values, corresponding to high positive surface charges, cannot be obtained in EAN. In contrast, for citrate-coated particles, the pH in EAN (6.5) is close to that in water (7.5) and almost equal to the third pK of citrate (pK_3 = 6.6 in EAN, see SI for details). This indicates that the particles likely maintain a negative surface charge in EAN.

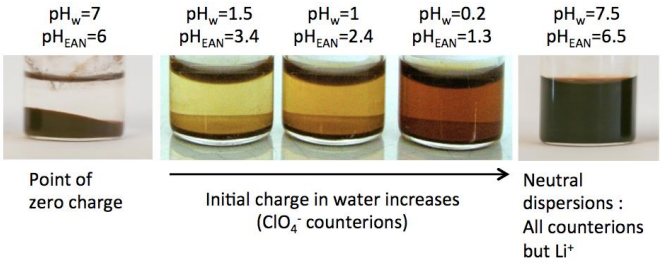

Figure 1: Typical aspects of ferrofluid samples in EAN: totally flocculated at the point of zero charge (left); the concentration of dispersed nanoparticles in the supernatant increases with the nanoparticles surface charge, as shown by its color (middle, case of acidic particles); for higher volume fractions in the supernatant, flocs at the bottom are no longer visible on the photo (right, case of neutral dispersions with citrate coating). pH_w: pH in water samples; pH_{EAN}: pH in EAN samples.

Let us now examine the influence of the nature of counterions. In acidic medium, as mentioned earlier, the surface of the particles is positively charged, and must be compensated by the presence of negative counterions. In this work, three counterions were used for the acidic dispersions: nitrate NO_3^{-}, perchlorate ClO_4^{-} and benzenesulfonate BS^{-}. Upon transfer from water to EAN, partial dispersions are obtained with NO_3^{-} and ClO_4^{-}, the dispersed fraction being higher with perchlorate, whereas particles flocculate with BS^{-}.

In neutral medium, citrate-coated nanoparticles have a negatively charged surface, and several types of positive counterions were used to counterbalance such charge. Using the alkaline series (Li^{+}, Na^{+}, K^{+} and Cs^{+}) and various ammonium derivatives (NH_4^{+}, ethylammonium EtA^{+}, and tetramethylammonium TMA^{+}) allowed to probe the influence of cation size and polarizability, whereas the influence of valence was investigated using the divalent Ca^{2+} counterion. As a result, with all monovalent counterions, the particles are well dispersed in water, and they are successfully redispersed in EAN after freeze-drying, with the only exception being Li^{+} in EAN. Indeed, in the case of lithium counterion, upon transfer to the IL the sample is initially flocculated; the supernatant progressively darkens, indicating slow re-dispersion of the particles over a few days. Finally, in the case of Ca^{2+}, even the initial aqueous dispersions are flocculated; quite surprisingly, upon transfer to EAN, slow redispersion occurs. Such slow redispersion observed for the Li^{+} and Ca^{2+} samples represents a quite unusual phenomenon in colloidal systems, and may reflect a gradual reorganization of the interface.

Determining the iron content in the supernatant by flame atomic absorption spectroscopy (FAAS) provides the volume fraction of particles Φ_{NP}. All supernatants display similar nanoparticles concentrations (equal to about 70-80% of the maximal expectable volume fraction; the remaining 30-20% of particles precipitate); exceptions are lithium (40%) and calcium

(60%). Such results clearly reveal a significant influence of counterions nature on the dispersability of colloidal maghemite particles in EAN.

In order to obtain more detailed information about the exact role of particle charge and counterion nature for monovalent species, we performed a structural analysis on the most concentrated dispersions: scattering experiments were carried out on the supernatants of neutral dispersions in both water and EAN. DLS measurements (see SI for technical details) revealed similar particle sizes in water and EAN, except for Li^+ for which aggregates were observed soon after transfer in EAN. These aggregates disappeared over time, and the final average size was lower than for the other counterions. In all cases, due to the high polydispersity of our samples, detailed analysis of DLS results is not straightforward and we then concentrated our efforts on Small Angle Neutron Scattering (SANS).

SANS measurements were performed on the PACE spectrometer at the LLB facility (CEA Saclay, France). Three different configurations were used (neutron wavelength λ = 13 Å, sample to detector distance d = 4.7 m; λ = 4.5 Å, d = 4.7 m; λ = 4.5 Å, d = 1.1 m) giving access to a q-range extending from $3.2 \cdot 10^{-3}$ $Å^{-1}$ down to 0.4 $Å^{-1}$. Samples were conditioned in quartz cells of 1 mm inner thickness. Standard correction procedures were implemented[22] using the Pasinet software (available free of charge at http://didier.lairez.fr/) in order to obtain the scattered intensity in absolute scale (cm^{-1}) (see SI for details).

Figure 2a presents the scattering curves obtained for all monovalent counterions in EAN, together with two aqueous dispersions obtained for Na^+ and Li^+: the scattered intensities, normalized by the NP volume fractions, are practically superposed except for the Li^+ sample, which is different from the others. Data analysis allows to obtain (i) the volume fraction in particles from the calculation of the scattering invariant; (ii) particle size and (iii) possible interactions between them. This is achieved by fitting the whole I(q) curve using a combination of a form factor of spheres with a lognormal size distribution and a structure factor.

Firstly, the volume fractions deduced from the invariant are in very good agreement with the values measured by FAAS (see SI for all the values). Secondly, the curves can be convincingly fitted by using a pure form factor (no interactions). This reveals that, in the experimental conditions investigated here, a stable dispersed state of the colloids is obtained in all cases. Given the low volume fraction of the dispersions (Φ_{NP} = 0.4% to Φ_{NP} = 1%, see SI), the interparticle interactions were undetectable in all cases, as evidenced by the lack of apparent structure factor.

Still, a detailed inspection of the different scattering curves and associated fits reveals additional features. Basically, three situations can be distinguished (Figure 2b):

(1) Samples in water (Na^+ or Li^+ counterion), for which the fit results yield an average diameter d_0 = 5.6 nm with a polydispersity index σ = 0.44;

(2) Samples in EAN with all counterions but Li^+, for which d_0 = 5.2 nm and σ = 0.43;

(3) Sample in EAN with Li^+ as counterion, for which d_0 = 4.6 nm and σ = 0.40.

Such results clearly prove that, upon transfer from water to EAN, in the case of Li^+ the smaller particles are more easily dispersed than larger ones (that remain in the flocculated fraction). Such an effect is also detectable, although weaker, for the other counterions in EAN. Furthermore, the nature of the counterion clearly affects the solid/liquid interface in EAN. Indeed, if the initial counterion of citrate had been fully replaced by EtA^+ (*i.e.*, the cation of EAN), which is present in large excess, all systems would display similar behaviour and structure. Consequently, the differences observed in the specific case of Li^+ prove that the counterions of the initial aqueous system remain close to the solid surface in EAN.

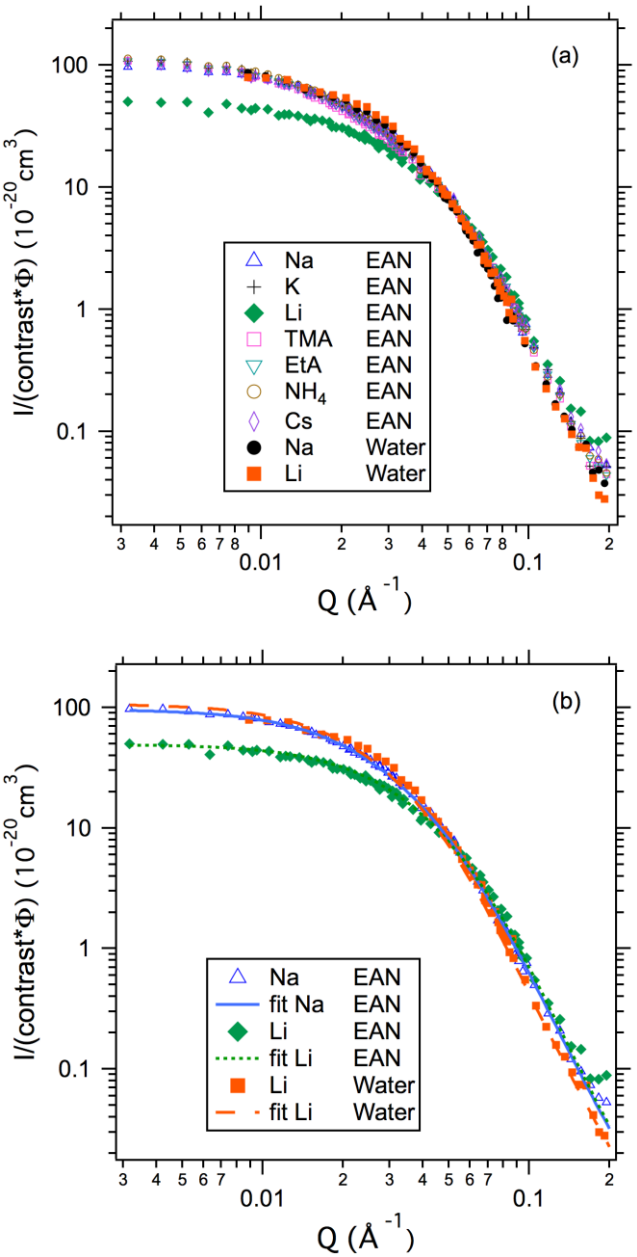

Figure 2: SANS intensity normalized by contrast and volume fraction for negatively charged citrate-coated particles with various counterions (indicated on the graphs). Upper plot (a): all data. Bottom plot (b): one representative curve for each case and the corresponding fit (see text for details).

Let us now turn to the interparticle interactions for the system in study. The colloidal stability observed on the macroscopic scale as well as the microstructure determined by SANS suggest that some interparticle repulsions must exist in EAN to counterbalance the existing attractive forces. Indeed, the van der Waals and dipolar magnetic attractions between maghemite NP

in EAN are expected to be respectively close and equal to the values in water. Since these two attractive interactions strongly increase with particle radius but do not depend on the counterion, the intensity of repulsions required for stabilization decreases when decreasing particles size. These repulsions appear here to be counterion-dependent, being of lower intensity in the case of lithium ions as only the smallest particles are dispersed.

The origin of such repulsion was questioned in some of the few works on IL-based colloids. The most common interpretation involves a layered organization of the IL at the nanoparticle/IL interface. IL layering on a thickness of 2-8 ion pairs has been experimentally evidenced by recent AFM[23,24] and X-ray reflectivity[25] measurements carried out on flat charged surfaces. In parallel, several molecular dynamics simulations also revealed IL layering at both flat interfaces such as solid electrodes.[26] Experimental and simulation studies showed that the relevant parameters controlling layering are the value of the surface charge, the nature, size and flexibility of the IL ions, and the roughness of the surface.

Only a few recent works consider the presence of added salt on the flat solid/IL interface. The addition of LiCl in the IL, studied by AFM,[27,28] has a strong influence on the structuration of the interface, reducing the repulsion between tip and gold surface.

Even fewer studies deal with curved surfaces. While simulation works were able to show the presence of IL layering on carbon nanotubes,[26] no direct experimental evidence can be obtained on nanoparticles. Nevertheless, the presence of Li^+ at the interface in a silica/IL colloidal dispersion has been proven to modify the microstructure of the system.[29]

In the present work, in the case of Li^+, the counterion seems to play a similar role as in previous works[29]: its concentration being too low to attribute the recorded effects to bulk modifications, the cation is most probably located at the NP/EAN interface. Unfortunately, there have not yet been any studies involving other cations than Li^+.

The results reported here appear consistent with a strong influence of surface charge and counterion nature on the repulsive interactions between particles. This is consistent with the studies concerning flat surfaces, suggesting that the aforementioned parameters appear to be significant even for nanoparticles whose surfaces exhibit defects and inhomogeneities.

Conclusions

The experiments reported in the present letter clearly show that the dispersability of nanoparticles in the ionic liquid EAN is influenced by both the charge value and the nature of the counterions compensating this charge. Fine-tuning both parameters could then allow better control of the structure of dispersions in ILs (aggregates, gels…). The specific role of lithium ions evidenced in the present work may bear particular significance considering the numerous electrochemical applications of ILs. Still, many open questions are pending, particularly concerning the influence of the nature of the original counterions, considering their low concentration. This could be tentatively linked to the amount of residual water present in the ILs, which may mediate the structuration of the interface through a counterion-dependent hydration of the nanoparticles' surface. Furthermore, a clearer understanding of interparticle interactions in ionic liquids should be obtained in future studies by varying nanoparticle size as well as volume fraction.

Acknowledgements

We acknowledge funding from Émergence-UPMC-2010 research program. This work has been supported by the Region Ile-de-France in the framework of C'Nano IdF. C'Nano IdF is the nanoscience competence center of Paris Region, supported by CNRS, CEA, MESR and Region Ile-de-France. We thank D. Baillon, J. Jestin, P. Levitz, A. Michel, L. Michot and D. Talbot for their contributions to this work.

Notes and references

[a] Laboratoire PECSA, UPMC – ESPCI – CNRS, 4 place Jussieu, 75005 Paris, France.

[b] Laboratoire Léon Brillouin, CEA Saclay, 91191 Gif-sur-Yvette, France.

Electronic Supplementary Information (ESI) available: experimental details on the synthesis of EAN; pH determinations and dissociation constants of citric acid in EAN; DLS and SANS technical details. See DOI: 10.1039/c000000x/

1. T. Torimoto, T. Tsuda, K. Okazaki, and S. Kuwabata, *Adv. Mater.*, 2010, **22**, 1196–1221.
2. Z. Li, Z. Jia, Y. Luan, and T. Mu, *Curr. Opin. Solid State Mater. Sci.*, 2008, **12**, 1–8.
3. Q. Zhang, S. Zhang, and Y. Deng, *Green Chem.*, 2011, **13**, 2619.
4. E. B. Fox, A. E. Visser, N. J. Bridges, and J. W. Amoroso, *Energy Fuels*, 2013, **27**, 3385–3393.
5. J. Le Bideau, L. Viau, and A. Vioux, *Chem. Soc. Rev.*, 2011, **40**, 907.
6. H. Yang, C. Yu, Q. Song, Y. Xia, F. Li, Z. Chen, X. Li, T. Yi, and C. Huang, *Chem. Mater.*, 2006, **18**, 5173–5177.
7. D. S. Jacob, A. Rothschild, H. L. Tuller, and A. Gedanken, *Ultrason. Sonochem.*, 2010, **17**, 726–729.
8. D. Zhao, Z. Fei, W. H. Ang, and P. J. Dyson, *Small*, 2006, **2**, 879–883.
9. N. Jain, X. Zhang, B. S. Hawkett, and G. G. Warr, *ACS Appl. Mater. Interfaces*, 2011, **3**, 662–667.
10. G.-T. Wei, Z. Yang, C.-Y. Lee, H.-Y. Yang, and C. R. C. Wang, *J. Am. Chem. Soc.*, 2004, **126**, 5036–5037.
11. L. Rodríguez-Arco, M. T. López-López, F. González-Caballero, and J. D. G. Durán, *J. Colloid Interface Sci.*, 2011, **357**, 252–254.
12. J. A. Smith, O. Werzer, G. B. Webber, G. G. Warr, and R. Atkin, *J. Phys. Chem. Lett.*, 2010, **1**, 64–68.
13. K. Ueno, A. Inaba, M. Kondoh, and M. Watanabe, *Langmuir*, 2008, **24**, 5253–5259.
14. F. C. C. Oliveira, L. M. Rossi, R. F. Jardim, and J. C. Rubim, *J. Phys. Chem. C*, 2009, **113**, 8566–8572.
15. M.-A. Neouze, *J. Mater. Chem.*, 2010, **20**, 9593.
16. R. Kanzaki, K. Uchida, S. Hara, Y. Umebayashi, S. Ishiguro, and S. Nomura, *Chem. Lett.*, 2007, **36**, 684–685.
17. D. F. Evans, A. Yamauchi, R. Roman, and E. Z. Casassa, *J. Colloid Interface Sci.*, 1982, **88**, 89–96.
18. R. Massart, *IEEE Trans. Magn.*, 1981, **2**, 1247.
19. I. T. Lucas, S. Durand-Vidal, E. Dubois, J. Chevalet, and P. Turq, *J. Phys. Chem. C*, 2007, **111**, 18568–18576.
20. S. Odenbach, *Colloidal Magnetic Fluids: Basics, Development and Application of Ferrofluids*, Springer-Verlag Berlin Heidelberg, 2009.
21. F. Cousin, E. Dubois, and V. Cabuil, *Phys. Rev. E*, 2003, **68**.

22. A. Brûlet, D. Lairez, A. Lapp, and J.-P. Cotton, *J. Appl. Crystallogr.*, 2007, **40**, 165–177.
23. R. G. Horn, D. F. Evans, and B. W. Ninham, *J. Phys. Chem.*, 1988, **92**, 3531–3537.
24. R. Hayes, G. G. Warr, and R. Atkin, *Phys. Chem. Chem. Phys.*, 2010, **12**, 1709.
25. M. Mezger, H. Schroder, H. Reichert, S. Schramm, J. S. Okasinski, S. Schoder, V. Honkimaki, M. Deutsch, B. M. Ocko, J. Ralston, M. Rohwerder, M. Stratmann, and H. Dosch, *Science*, 2008, **322**, 424–428.
26. G. Feng, R. Qiao, J. Huang, S. Dai, B. G. Sumpter, and V. Meunier, *Phys. Chem. Chem. Phys.*, 2011, **13**, 1152.
27. F. Endres, N. Borisenko, S. Z. El Abedin, R. Hayes, and R. Atkin, *Faraday Discuss.*, 2012, **154**, 221.
28. R. Hayes, N. Borisenko, B. Corr, G. B. Webber, F. Endres, and R. Atkin, *Chem. Commun.*, 2012, **48**, 10246.
29. J. Nordström, L. Aguilera, and A. Matic, *Langmuir*, 2012, **28**, 4080–4085.